scientific reports

OPEN

Temporal variation characteristics in the association between climate and vegetation in Northwest China

Shijun Zheng[1], Dailiang Peng[2,3]✉, Bing Zhang[2,3,4], Le Yu[1]✉, Yuhao Pan[2,3], Yan Wang[5], Xuxiang Feng[6] & Changyong Dou[2,3]

Northwest China has undergone notable alterations in climate and vegetation growth in recent decades. Nevertheless, uncertainties persist concerning the response of different vegetation types to climate change and the underlying mechanisms. This study utilized the Normalized Difference Vegetation Index (NDVI) and three sets of meteorological data to investigate the interannual variations in the association between vegetation and climate (specifically precipitation and temperature) from 1982 to 2015. Several conclusions were drawn. (1) $R_{NDVI-GP}$ (relationship between Growing Season NDVI and precipitation) decreased significantly across all vegetation, while $R_{NDVI-GT}$ (relationship between Growing Season NDVI and temperature) showed an insignificant increase. (2) Trends of $R_{NDVI-GP}$ and $R_{NDVI-GT}$ exhibited great variations across various types of vegetation, with forests displaying notable downward trends in both indices. The grassland exhibited a declining trend in $R_{NDVI-GP}$ but an insignificant increase in $R_{NDVI-GT}$, while no significant temporal changes in $R_{NDVI-GP}$ or $R_{NDVI-GT}$ were observed in the barren land. (3) The fluctuations in $R_{NDVI-GP}$ and $R_{NDVI-GT}$ closely aligned with variations in drought conditions. Specifically, in regions characterized by VPD (vapor pressure deficit) trends less than 0.02 hpa/yr, which are predominantly grasslands, a rise in SWV (soil water volume) tended to cause a reduction in $R_{NDVI-GP}$ but an increase in $R_{NDVI-GT}$. However, a more negative trend in SWV was associated with a more negative trend in both $R_{NDVI-GP}$ and $R_{NDVI-GT}$ when the VPD trend exceeded 0.02 hPa/yr, primarily in forests. Our results underscore the variability in the relationship between climate change and vegetation across different vegetation types, as well as the role of drought in modulating these associations.

Keywords Vegetation, Climate, NDVI, Relationship, Northwest China

Land vegetation serves as a crucial conduit that connects the soil, atmosphere, and water cycle, and plays a critical role in regulating the exchange of water and heat[1–3]. Comprehending the interactions between climate and vegetation is important for ecological restoration[4]. Considerable research efforts are aimed at investigating the response of vegetation growth to climate change[5–9], with a predominant focus on elucidating the promoting or inhibitory effects of climate variables, including temperature or precipitation, on vegetation dynamics. It has been found that the correlation between temperature and vegetation productivity may vary over time due to other environmental constraints[10,11], indicating that the interaction between climate and vegetation may undergo modifications as a result of vegetation's self-adjustment or shifts in the surrounding ecosystem. Exploring these changes in the vegetation-climate correlation and their underlying mechanisms is of significant importance for maintaining ecosystem stability.

The changing correlation between climate and vegetation has recently gained some attention. For instance, Wang, et al.[12] observed a weakening correlation between vegetation and temperature across China over the past 34 years. A study in Australia revealed a decreasing precipitation threshold necessary for vegetation growth[13]. Keenan and Riley[14] investigated how vegetation cover responded to temperature variations and noted

[1]Ministry of Education Key Laboratory for Earth System Modeling, Department of Earth System Science, Tsinghua University, Beijing 100084, China. [2]Key Laboratory of Digital Earth Science, Aerospace Information Research Institute, Chinese Academy of Sciences, Beijing 100094, China. [3]International Research Center of Big Data for Sustainable Development Goals, Beijing 100094, China. [4]University of Chinese Academy of Sciences, Beijing 100049, China. [5]Department of Land Surveying and Geo-Informatics, The Hong Kong Polytechnic University, Hong Kong 999077, China. [6]China Remote Sensing Satellite Ground Station (RSGS), Aerospace Information Research Institute, Chinese Academy of Sciences, Beijing 100094, China. ✉email: pengdl@aircas.ac.cn; leyu@tsinghua.edu.cn

1

a diminishing impact of temperature constraints over time. Zhao et al.[15] reported an enhanced association between climate change and vegetation index in Northwest China over the past 34 years. Nevertheless, these studies have primarily focused on recognizing the changes in the relationship between climate and vegetation. Uncertainties remain regarding the underlying drivers and mechanisms that regulate these changes in the relationship. Moreover, current research on the changing relationship between climate and vegetation often fails to take into account the differences in vegetation types. Extensive documentation exists on the influencing mechanisms of vegetation dynamics in diverse vegetation types[16–23], indicating potential variations in the patterns of interactions between climate and vegetation across different land cover types.

Northwest China is distinguished by extensive regions encompassing diverse land cover types, including grasslands, forests, and barren lands with sparse vegetation. Since the early 1980s, multiple studies have highlighted the presence of warmer and more humid conditions in this area[24–30]. Furthermore, notable alterations in vegetation growth have also been documented in recent decades within this region[31,32]. Yet, there is limited research on the changing relationship between climate and vegetation in Northwest China. Consequently, Northwest China provides an optimal context for investigating the evolving dynamics of the interaction between climate conditions and vegetation patterns across a range of vegetation types.

In this study, we utilized satellite-based normalized difference vegetation index (NDVI) data along with climate observations from three distinct sources (refer to the Methods section) to investigate the responses of various vegetation types in Northwest China to climate variations (temperature and precipitation). Additionally, we examined the temporal variation characteristics of the relationship between vegetation and climate. Furthermore, we performed an attribution analysis to determine the cause of this relationship's shifting trend. Our research will enhance the comprehension of the correlation between vegetation and climate, and concurrently provide a theoretical basis for safeguarding the ecological security of Northwest China.

Methodology

Study area

This study focuses on northwest China (Fig. 1a). Located in the interior of Eurasia, the altitude of this region ranges from − 152 to 8058 m, with the majority of areas situated at elevations exceeding 1000 m. The intricate topography hinders the long-distance transport of oceanic moisture across mountain barriers, resulting in an arid climate. The primary land cover types in this region include forest, grassland, and barren land (areas with an average annual NDVI below 0.1 were excluded to eliminate non-vegetated regions, hence the barren land here represents areas with sparse vegetation). Forest is predominantly concentrated in southern Shaanxi, while grassland is primarily distributed in the southern Qinghai Plateau, as well as the Qilian Mountains, Tianshan Mountains, and Altai Mountains (Fig. 1b). The distribution of NDVI and precipitation here demonstrates a coherent pattern, with notably elevated values predominantly localized in the southern areas of Qinghai and Shaanxi (Fig. 1c,d). This alignment suggests that precipitation is the primary climatic factor influencing vegetation growth under dry conditions[33,34]. The pronounced temperature disparities in this area stem from altitude-related influences
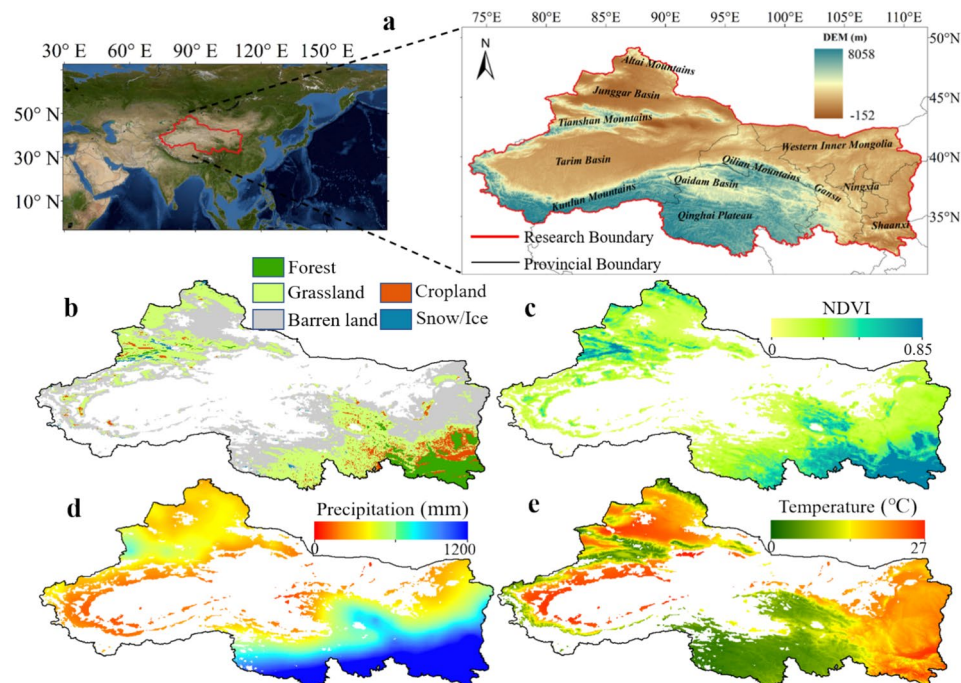
Figure 1. Study area. (**a**) The location and elevation of the study area, (**b**) land cover map, and spatial distribution of Growing Season (**c**) NDVI, (**d**) precipitation and (**e**) temperature. As the areas with an average annual NDVI of less than 0.1 were removed, the barren land in (**b**) represents sparse vegetation.

(Fig. 1e). High-altitude regions like the Qinghai Plateau, Qilian Mountains, Tianshan Mountains, and Altai Mountains exhibit growing season temperatures averaging below 5 °C. Conversely, most other areas have average temperatures surpassing 15 °C, with specific areas in southern Shaanxi, the Junggar Basin, and the Tarim Basin even exceeding 25 °C.

Data sets

Three sets of climate data were employed in our analysis. The first dataset comprises temperature and precipitation grid data obtained through interpolation of meteorological station data at a spatial resolution of 1 kilometers[25], denoted as "Interp". Additionally, we utilized temperature and precipitation data from the Climatic Research Unit (CRU) Time Series 4.01[35], with a resolution of 0.5°. Lastly, the ERA5-land reanalysis dataset with a resolution of 0.1° was also utilized[36], encompassing climate variables such as temperature, precipitation, shortwave radiation (SR), dew point temperature (DT), surface pressure (SP), and soil water volume at a depth of 0–7 cm (SWV). Among these climate variables, SR was utilized as a controlled variable in partial correlation analysis to mitigate its impact on the inter-annual changes of NDVI when examining the relationship between NDVI, temperature, and precipitation. The variables DT and SP were used for calculating vapor pressure deficit (VPD) and, in conjunction with SWV, to investigate the impact of drought on the correlation between temperature, precipitation, and NDVI. As all meteorological data were at monthly scale, we transformed them into the Growing Season (GS) by aggregating precipitation and averaging temperature, shortwave radiation (SR), vapor pressure deficit (VPD), and soil water volume (SWV). The Growing Season was defined as April to October. Subsequently, all climate variables were resampled to a 0.05° resolution through bilinear interpolation to align with the resolution of the land cover data. Additionally, all variable raster data in this study were georeferenced using the WGS84 coordinate system with a longitude-latitude projection. VPD was calculated by the following formulas[37]:

$$SVP = 6.112 \times \left(1 + 7 \times 10^{-4} + 3.46 \times 10^{-6} SP\right) \times e^{\frac{17.67 T_a}{T_a + 243.5}} \tag{1}$$

$$AVP = 6.112 \times \left(1 + 7 \times 10^{-4} + 3.46 \times 10^{-6} SP\right) \times e^{\frac{17.67 T_d}{T_d + 243.5}} \tag{2}$$

$$VPD = SVP - AVP \tag{3}$$

where SVP and AVP are vapor pressure and actual vapor pressure (kPa), respectively. T_a is the air temperature (°C). T_d is the dew point temperature (°C). SP is the surface pressure (hPa).

The NDVI is a widely used indicator of vegetation greenness, commonly employed in studies investigating changes in vegetation greenness and their responses to climate variability[38]. In this study, NDVI data spanning the period 1982–2015 was obtained from the Global Inventory Modeling and Mapping Studies NDVI third generation (GIMMS NDVI3g) (available in "https://climatedataguide.ucar.edu/climate-data/ndvi-normalized-difference-vegetation-index-3rd-generation-nasagfsc-gimms"), which has been shown to be one of the best products for monitoring temporal changes in vegetation[39,40]. This dataset, derived from NOAA's Advanced Very High Resolution Radiometer (AVHRR) sensor, provides average NDVI values by filtering out atmospheric disturbances, snow, and other interferences, with a temporal resolution of 15 days and a spatial resolution of approximately 8 km. To aggregate the biweekly NDVI data into monthly intervals, the Maximum Value Composite (MVC)[41] approach was employed to eliminate noise from cloud and atmospheric conditions effectively. Subsequently, Growing Season (GS) NDVI was calculated by averaging the monthly NDVI values while excluding regions with an average annual NDVI below 0.1 to eliminate non-vegetated areas[42,43]. Moreover, the NDVI data was also resampled to a spatial resolution of 0.05° using bilinear interpolation to match the resolution of the land cover data.

The land cover data, characterized by a spatial resolution of 0.05°, was obtained from GLASS-GLC (Global Land Surface Satellite—global land cover)[44] and can be accessed at "https://doi.org/10.1594/PANGAEA.913496". It's categorized into seven classes: cropland, forest, grassland, shrubland, tundra, barren land, and snow/ice. This dataset has been extensively employed in various academic studies[45–47].

Partial correlation analysis

Prior to the analysis, the linear trends in both the NDVI and climate time series were detrended using the least squares method. The relationship between precipitation (temperature) and NDVI is assessed by computing the partial correlation coefficient between GS precipitation (temperature) and GS NDVI, while statistically controlling for interannual variation in GS temperature (precipitation) and GS radiation. The calculation of the partial correlation coefficient is depicted in formula (4)[48].

$$R_{x_j y} = \frac{-c_{jy}}{\sqrt{c_{jj} c_{yy}}} \tag{4}$$

where $R_{x_j y}$ is the partial correlation coefficient between the j th independent variable and the dependent variable y, c is the corresponding element in the inverse matrix of the correlation coefficient matrix. The statistical significance of the partial correlations was calculated using the t-test shown in formula (5)[49] with the significance level set to 0.05:

$$t_{xy,z} = \frac{r_{xy,z}}{\sqrt{1 - r_{xy,z}^2}} \sqrt{n - m - 1}$$

(5)

here m is the number of independent variables and n is the number of samples.

Results
### The correlation of climate and NDVI

The Northwest China witnessed a remarkable shift towards warmer and more humid climate from 1982 to 2015, characterized by an overall temperature rise across all regions and a precipitation increase in the majority of areas (Fig. S1a,b). The primary regions experiencing a decrease in precipitation are the forests in the southern Shaanxi and the barren lands in the northern part of Xinjiang (Figs. 1a and S1b).

We utilized various sets of meteorological data to compute the partial correlation coefficients between temperature, precipitation, and NDVI, as depicted in Fig. 2. Across the majority of areas, NDVI exhibited a positive correlation with precipitation, particularly in sparsely vegetated regions. Remarkably, in the grassland areas of southern Qinghai Plateau, NDVI displayed a significant negative correlation with precipitation. Except for specific regions like the Tianshan Mountains and southern Qinghai Plateau, a negative correlation was observed between NDVI and temperature in a significant portion of northwest China, particularly in sparsely vegetated areas. The partial correlation analysis conducted with Interp and ERA5 meteorological data revealed a subtle positive correlation between temperature and NDVI in some barren regions situated in the northern part of the Tianshan Mountains (Fig. 2b, f). This may potentially be attributed to the accelerated melting of high mountain glaciers caused by rising temperatures, subsequently facilitating the growth of vegetation[50].

The correlation between climate and NDVI is closely linked to the spatial distribution of climate in Northwest China. Generally, a strong correlation between NDVI and precipitation is observed in areas with low precipitation levels. However, as precipitation levels increase, the correlation gradually weakens, and may even become negative (Fig. 3a–c). This can be attributed to the high dependence of vegetation growth on precipitation in water-deficient areas, while vegetation growth in relatively humid regions shows less sensitivity to precipitation[51,52]. As a result, the correlation between NDVI and precipitation is more pronounced in areas with sparse vegetation and bare ground compared to grassland and forest. At low temperatures, there is a positive relationship between NDVI and temperature, which strengthens with increasing temperature. However, upon reaching a specific threshold, the
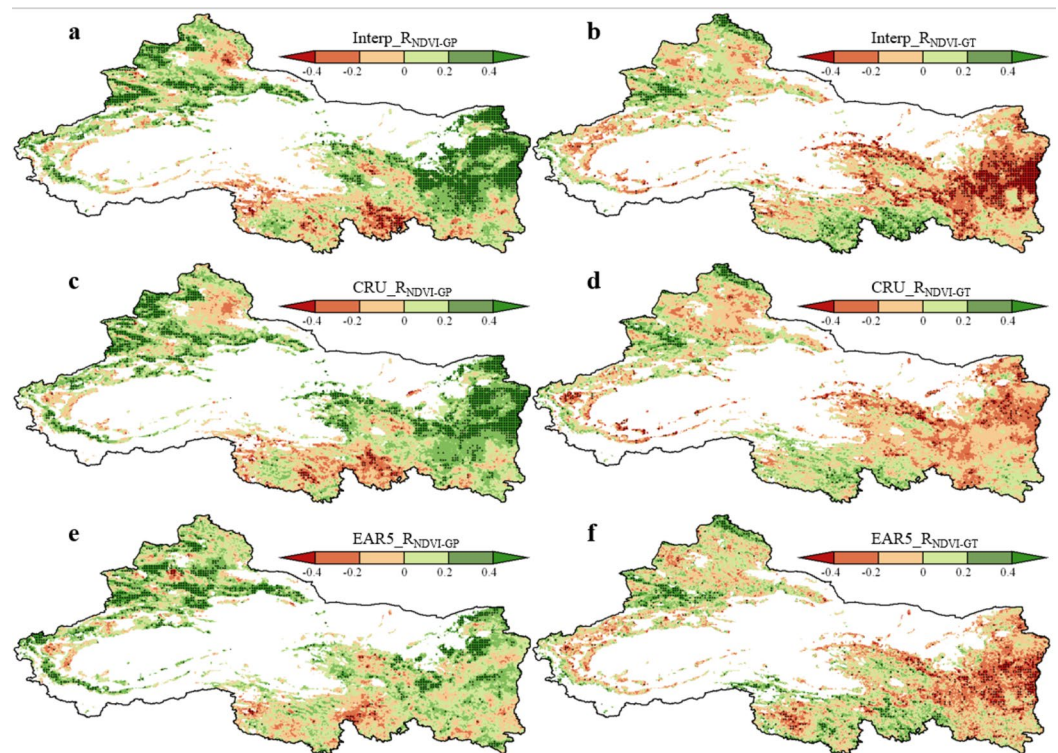
Figure 2. Spatial distribution of partial correlation of NDVI and climate. Partial correlation coefficient ($R_{NDVI-GP}$) between Growing Season NDVI and precipitation is calculated using climate data from Interp (**a**), CRU (**c**) and ERA5 (**e**). Partial correlation coefficient ($R_{NDVI-GT}$) between Growing Season NDVI and temperature is calculated using climate data from Interp (**b**), CRU (**d**) and ERA5 (**f**). The areas with an average annual NDVI of less than 0.1 were removed. All variables are detrended. To calculate the partial correlation of NDVI versus Growing Season precipitation (or temperature), temperature (or precipitation) and radiation are controlled for. The dots indicate the regions with significant relationship in $R_{NDVI-GP}$ (or $R_{NDVI-GT}$) ($P < 0.05$).
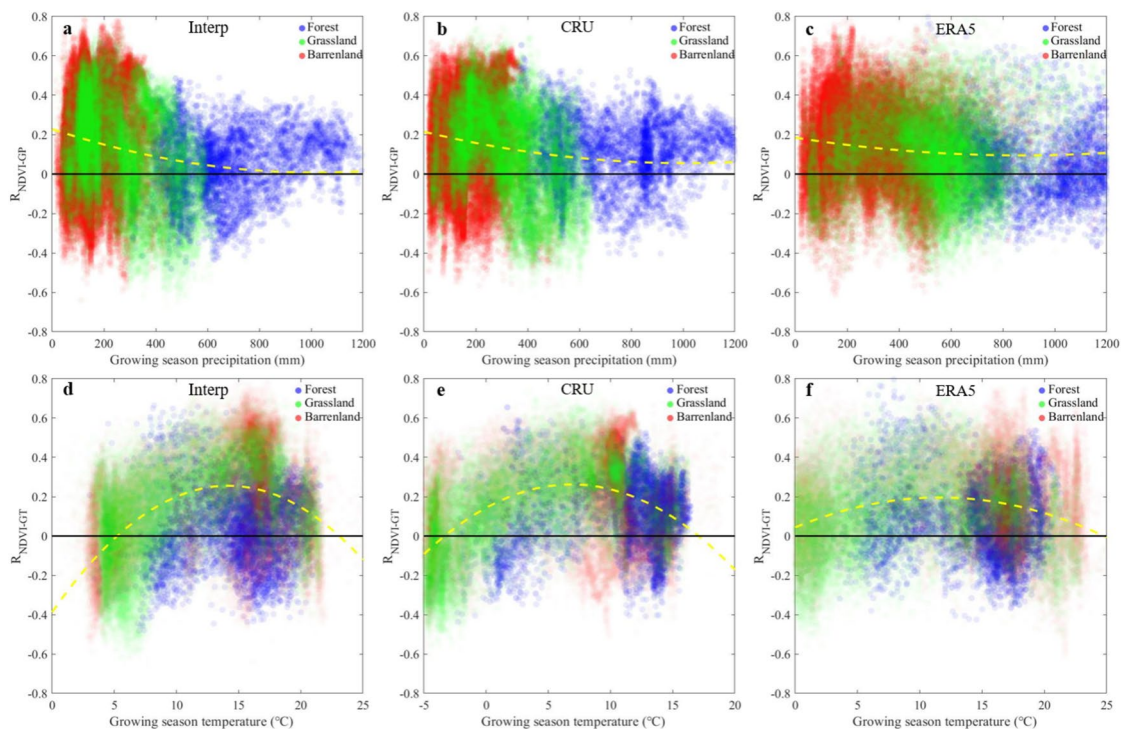
**Figure 3.** Scatter plots between $R_{NDVI-GP}$ and precipitation from Interp (**a**), CRU (**b**) and ERA5 (**c**), and scatter plots between $R_{NDVI-GT}$ and temperature from Interp (**d**), CRU (**e**) and ERA5 (**f**). Here, $R_{NDVI-GP}$ is the partial correlation coefficient between Growing Season NDVI and precipitation, and $R_{NDVI-GT}$ is the partial correlation coefficient between Growing Season NDVI and temperature (All variables are detrended). As the parts with NDVI < 0.1 are removed, the barren areas here represent sparse vegetation. The yellow dashed line is the quadratic fit for all the scatters.

correlation between NDVI and temperature weakens with further temperature elevation (Fig. 3d–f), signifying a potential decline or cessation of the current trend towards enhanced greening[53]. Prior studies have indicated that vegetation growth typically exhibits an optimal temperature, representing the temperature at which vegetation growth is most favorable[54,55]. In areas with lower temperatures, vegetation growth is highly sensitive to temperature variations, whereas in warmer regions, elevated temperatures can hinder vegetation growth. Consequently, grassland in high-altitude areas exhibits a positive correlation with temperature, whereas sparse vegetation on bare ground in warmer areas shows a negative correlation with temperature.

For some forested areas in Shaanxi, NDVI demonstrates a weak negative correlation with precipitation (Fig. 2a,c,e), potentially due to the elevation of solar radiation with decreasing precipitation in this region (Fig. S1b,e). To investigate the impact of solar radiation on vegetation productivity in Northwest China, we conducted an analysis on the partial correlations between interannual fluctuations in shortwave radiation and NDVI (Fig. S2). Increased radiation can enhance photosynthetic efficiency and promote vegetation growth, leading to a significant positive correlation between NDVI and radiation in forests (Fig. S2). However, high-altitude grasslands primarily exhibit a negative correlation with NDVI, possibly due to excessive radiation also raising transpiration rates and then causing soil moisture loss[56].

Trends in the relationship between climate and NDVI

The trends of $R_{NDVI-GP}$ and $R_{NDVI-GT}$ were calculated for overall vegetation areas, as well as individually for forest, grassland, and barren land, utilizing a sliding window approach along the time axis and relying on three sets of meteorological datasets, Interp, ERA5, and CRU. Figure 4 displays the outcomes derived from a 13-year sliding window, while Figs. S3–6 present additional analyses conducted with sliding windows of 9, 11, 15, and 17 years to bolster the reliability of the findings. The $R_{NDVI-GP}$ exhibited a notable decreasing trend for across all vegetation, with statistical significance ($P < 0.05$) observed in all cases except when utilizing Interp data with a 17-year sliding window. Specifically, the decline in $R_{NDVI-GP}$ within the forest was highly significant ($P < 0.01$ and $r < -0.75$ for all cases). In the grassland, a consistent downward trend in $R_{NDVI-GP}$ was evident ($P < 0.1$ for most cases), although with lower significance than in the forest. Conversely, there was no consistent trend, either upward or downward, observed in $R_{NDVI-GP}$ for barren lands, and the results lacked statistical significance. The trend analyses of $R_{NDVI-GT}$ show distinct disparities compared to those of $R_{NDVI-GP}$. Across all vegetation, the majority of $R_{NDVI-GT}$ trends demonstrate a non-significant increase. In the forest, $R_{NDVI-GT}$ exhibited a notable downward trend ($P < 0.05$ for most cases). More than two-thirds of cases demonstrate an increasing trend in the grassland, but the majority of them are not statistically significant. In the barren land, the trends of $R_{NDVI-GT}$, like $R_{NDVI-GP}$, lack a consistent directional pattern.
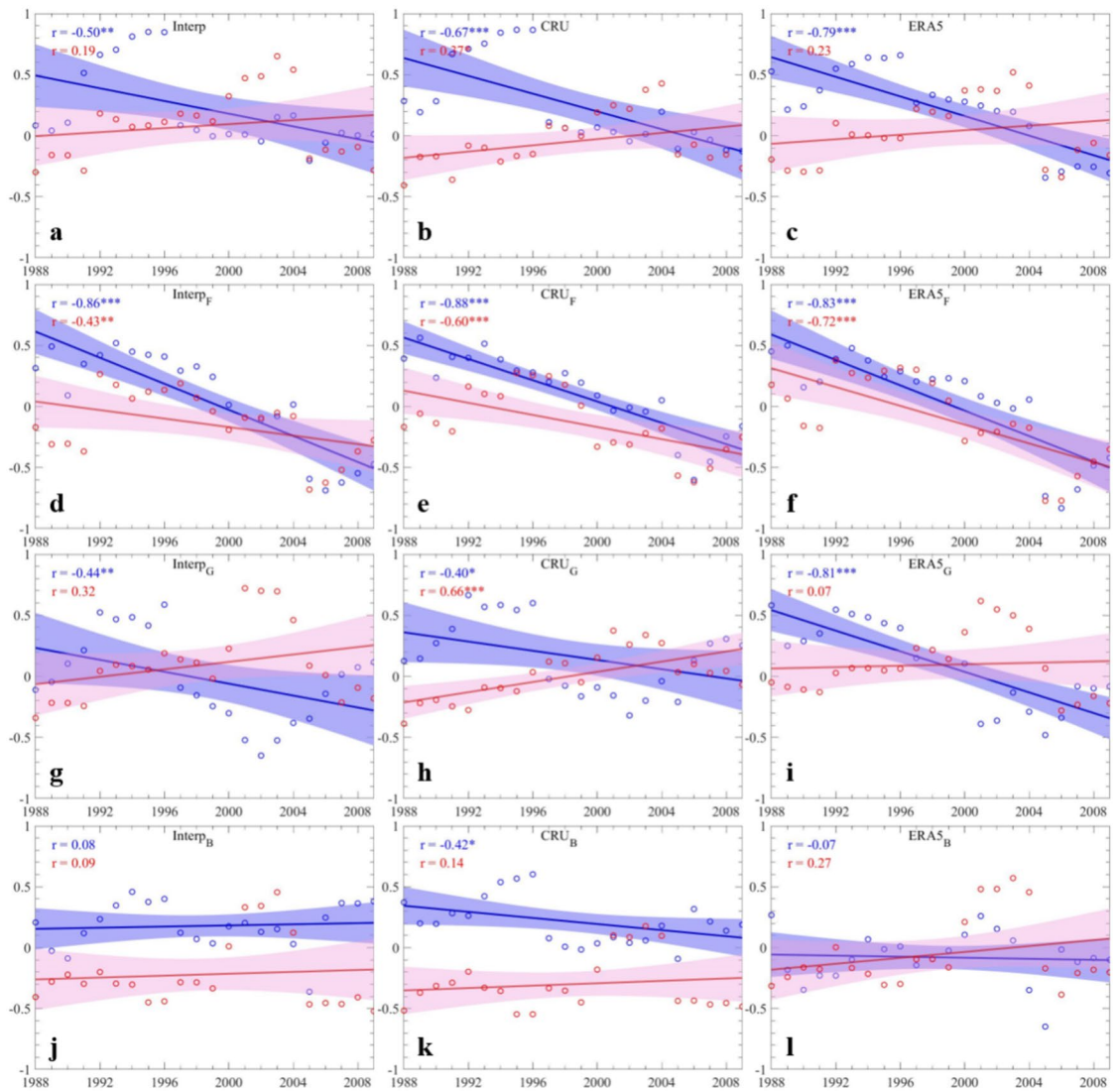
Figure 4. Changes in $R_{NDVI-GP}$ and $R_{NDVI-GT}$ at a 13-year sliding window. Here $R_{NDVI-GP}$ (or $R_{NDVI-GT}$) is the partial correlation coefficient between Growing Season NDVI and precipitation (or temperature), and is calculated using a 13-year sliding window during 1982–2015. All variables are detrended. The blue (or red) line represents the changes in $R_{NDVI-GP}$ (or $R_{NDVI-GT}$), and the shaded portion represents the confidence interval. Three types of climate data (Interp, CRU and ERA5) are used, corresponding to three columns. The first to fourth lines correspond to the following areas respectively: all vegetation areas except cropland, forest, grassland, and barren land (As the parts with NDVI < 0.1 are removed, the barren areas here represent sparse vegetation). The symbol of *, ** and *** in the upper right of the value of r indicate the significant trend at $P < 0.1$, $P < 0.05$ and $P < 0.01$ respectively.

The spatial distribution of trends in $R_{NDVI-GP}$ and $R_{NDVI-GT}$ using a 13-year sliding window was depicted in Fig. 5, while additional analyses conducted with sliding windows of 9, 11, 15, and 17 years were presented in Figs. S7–10, respectively. The consistent spatial patterns across different sliding windows validate the reliability of the experimental findings. Significant declines in $R_{NDVI-GP}$ were predominantly concentrated in the southern Shaanxi, northern Qinghai, and areas bordering the Tianshan Mountains, characterized by forests and grasslands. Conversely, regions with noteworthy increases in $R_{NDVI-GP}$ were observed in some interlaced areas of bare land and grassland in the northern part of Xinjiang and the western part of Qinghai. Significant decreases in $R_{NDVI-GT}$ have been observed in the majority of the eastern areas in the Northwest China. Conversely, the vast majority of areas in Qinghai exhibited a clear upward trend in $R_{NDVI-GT}$. Overall, $R_{NDVI-GP}$ and $R_{NDVI-GT}$ have exhibited a declining trend in approximately 81% and 71% of the total forest area in northwest China, respectively. In the grassland, $R_{NDVI-GP}$ showed a balanced distribution between positive and negative trends in terms of area, whereas $R_{NDVI-GT}$ displayed a predominant upward trend covering approximately 56% of the total grassland area. As for the barren land, the areas occupied by the positive and negative trends in $R_{NDVI-GP}$ or $R_{NDVI-GT}$ were roughly equivalent.
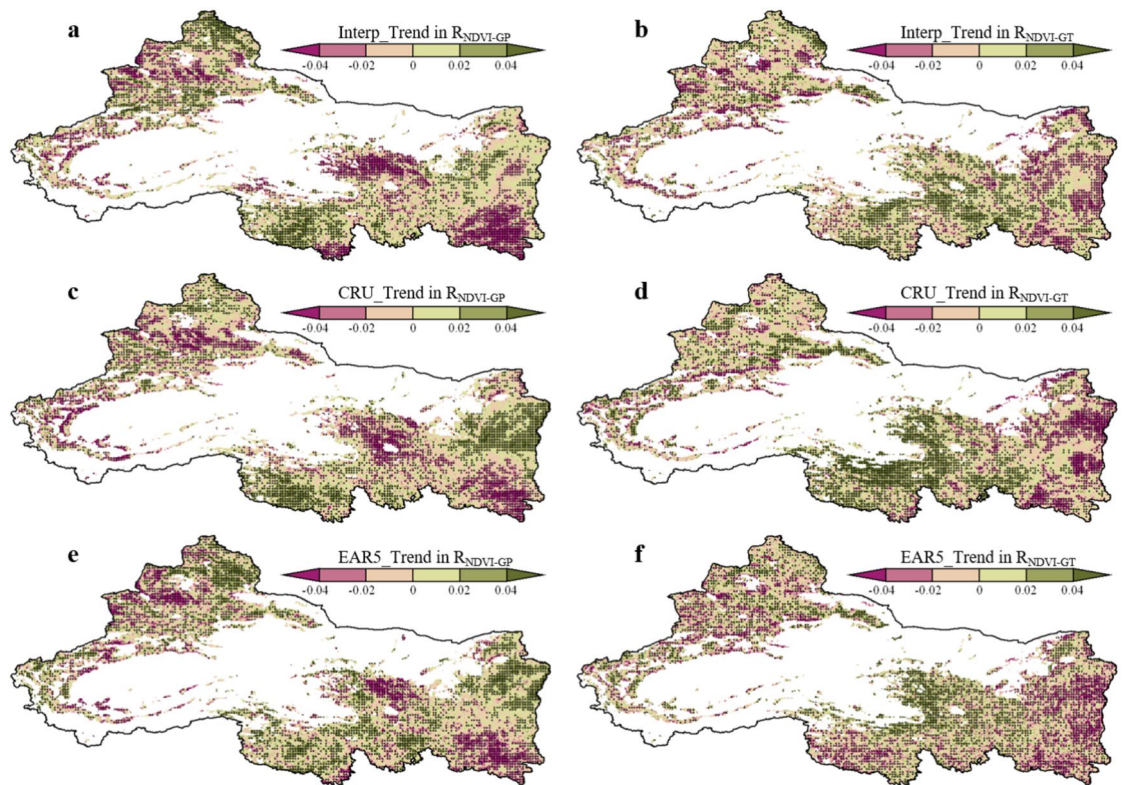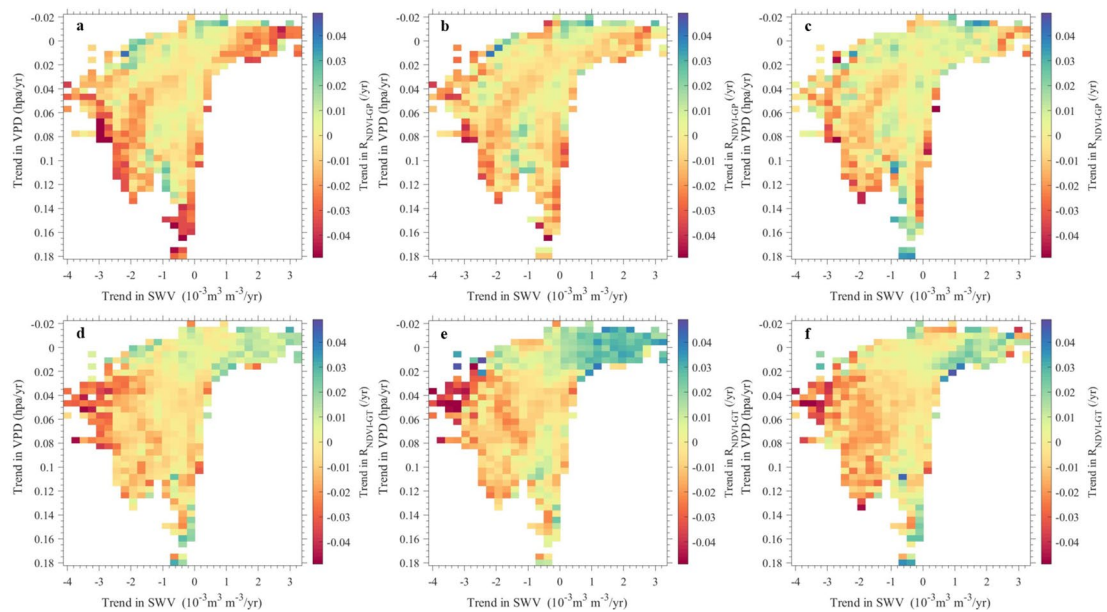
Figure 5. Spatial distribution of trends in $R_{NDVI-GP}$ and $R_{NDVI-GT}$ at a 13-year sliding window. Here, $R_{NDVI-GP}$ is the partial correlation coefficient between Growing Season NDVI and precipitation from Interp (**a**), CRU (**c**), and ERA5 (**e**); $R_{NDVI-GT}$ is the partial correlation coefficient between Growing Season NDVI and temperature from Interp (**b**), CRU (**d**), and ERA5 (**f**). They are calculated using a 13-year sliding window during 1982–2015. The areas with an average annual NDVI of less than 0.1 were removed. All variables are detrended. The dots indicate the regions with significant trend in $R_{NDVI-GP}$ (or $R_{NDVI-GT}$) ($P < 0.05$).

Discussion

This study utilizes various interannual sliding windows to compute the partial correlation coefficients between NDVI and temperature or precipitation, aiming to analyze the variations in the vegetation-climate relationship. While outcomes across different sliding windows are generally consistent, certain windows produce markedly different results. For instance, the association between grassland NDVI and temperature weakens under a 9-year sliding window, contrary to other windows (Fig. S3). Hence, this study considers results as robust conclusions only when a majority (defined as over two-thirds) of the sliding windows exhibit the same trend. Based on this criterion, no obvious temporal changes are observed in the relationship between vegetation and temperature or precipitation in barren land (Fig. 4 and Figs. S3–6). Prior research on the changes in the vegetation-climate correlation often relied on a single sliding window or a binary division of the study period for comparative analysis[12,56], leading to somewhat uncertain conclusions. In contrast, our research methodology effectively addresses such uncertainty.

It has been proposed that the reduced sensitivity of tree growth to temperature may be attributed to the potential impact of increased drought stress, which can modify the response of plant growth to temperature changes[53,57]. Decreases in soil water content and increases in atmospheric aridity resulting from drought can impede vegetation growth by affecting plant photosynthesis[56,58]. Therefore, this study investigated the roles of vapor pressure deficit (VPD) and soil water volume (SWV), as mechanisms that regulate the relationship between NDVI and temperature or precipitation. In Northwest China, particularly in forested regions, there was a general trend of increasing VPD and decreasing SWV from 1982 to 2015, except for Qinghai (Fig. S1c,d), indicating heightened drought severity in the region. The spatial distribution patterns of VPD and SWV trends closely resemble those of $R_{NDVI-GP}$ and $R_{NDVI-GT}$ trends (Fig. 5 and Fig. S1c,d). To further understand the functioning of these mechanisms, we present the trends of $R_{NDVI-GP}$ and $R_{NDVI-GT}$ plotted within the phase space of the trends in VPD and SWV using different sliding windows in Fig. 6 and Figs. S11–14. We observed that the VPD trend of 0.02 hPa/yr serves as a dividing line for the trends in SWV in Northwest China. When the VPD trend is less than 0.02 hPa/yr, the SWV trend exhibits variability, with regions showing a positive trend in SWV often exhibiting a negative trend in $R_{NDVI-GP}$, potentially indicating lower vegetation growth sensitivity to water availability under humid conditions[51,52]. Conversely, regions with a negative trend in SWV tend to demonstrate frequent negative trends in $R_{NDVI-GT}$, supporting the hypothesis that increased drought may diminish the temperature sensitivity of vegetation[57]. Furthermore, when the VPD trend exceeds 0.02 hPa/yr, the SWV trend tends to be negative. As the negative SWV trend intensifies, both $R_{NDVI-GP}$ and $R_{NDVI-GT}$ trends also become more negative, leading to the

Figure 6. Average trend of $R_{NDVI-GP}$ and $R_{NDVI-GT}$ at a 13-year sliding window in a climate phrase space. Here, $R_{NDVI-GP}$ is the partial correlation coefficient between GS NDVI and GS precipitation from Interp (**a**), CRU (**b**), and ERA5 (**c**); $R_{NDVI-GT}$ is the partial correlation coefficient between GS NDVI and GS temperature from Interp (**d**), CRU (**e**), and ERA5 (**f**). They are calculated using a 13-year sliding window during 1982–2015. All variables are detrended. The climate space is delineated by changes in GS soil water volume (SWV) and changes in vapor pressure deficit (VPD).

occurrence of maximum negative trends of $R_{NDVI-GT}$ and $R_{NDVI-GP}$ simultaneously in the forest (Figs. 5 and S1d). The alignment of $R_{NDVI-GP}$ and $R_{NDVI-GT}$ trends with the gradient of SWV trends suggests that this mechanism may play a crucial role in altering the relationship between vegetation and precipitation (or temperature).

Conclusions

This study aimed to investigate the interannual variations in the relationship between various types of vegetation (forest, grassland and barren land) and climate factors (precipitation and temperature) in Northwest China, and assessed the impact of drought on this relationship by examining the roles of VPD and SWV. Three sets of meteorological data and NDVI data were utilized for this analysis. Results revealed a significant decline in $R_{NDVI-GP}$ (the relationship between Growing Season NDVI and precipitation) across all vegetation in Northwest China, while $R_{NDVI-GT}$ (the relationship between Growing Season NDVI and temperature) showed an insignificant increase. The trends of $R_{NDVI-GP}$ and $R_{NDVI-GT}$ varied significantly among different vegetation types. Specifically, in the forest, both $R_{NDVI-GP}$ and $R_{NDVI-GT}$ exhibited a notable downward trend ($P < 0.05$). In the grassland, the $R_{NDVI-GP}$ displayed a decline trend with lower significance compared to the forest ($P < 0.1$), while $R_{NDVI-GT}$ exhibited a non-significant increasing trend. Sparse vegetation in the barren land did not show any clear temporal changes in $R_{NDVI-GP}$ or $R_{NDVI-GT.}$ The study found that fluctuations in $R_{NDVI-GP}$ and $R_{NDVI-GT}$ closely aligned with variations in drought conditions in Northwest China. In regions where VPD trends were below 0.02 hpa/yr, primarily characterized by grasslands, an increase in SWV tended to lead to a decrease in $R_{NDVI-GP}$ but an increase in $R_{NDVI-GT}$. However, when the VPD trend exceeded 0.02 hPa/yr, a more negative trend in SWV resulted in more negative trends in both $R_{NDVI-GP}$ and $R_{NDVI-GT}$.

Data availability

GIMMS NDVI data are available in http://data.tpdc.ac.cn/zh-hans/data/1cad1a63-ca8d-431a-b2b2-45d9916d860d/?q=GIMMS. The land cover data with a spatial resolution of 0.05° was obtained from GLASS-GLC and it's available at https://doi.org/10.1594/PANGAEA.913496. All the analyses are made using Python, and the code are available from the corresponding author on reasonable request.

References

1. Liu, Y. L. & Lei, H. M. Responses of natural vegetation dynamics to climate drivers in China from 1982 to 2011. *Remote Sens.* **7**, 10243–10268. https://doi.org/10.3390/rs70810243 (2015).
2. Zhong, L., Ma, Y. M., Salama, M. S. & Su, Z. B. Assessment of vegetation dynamics and their response to variations in precipitation and temperature in the Tibetan Plateau. *Clim. Change* **103**, 519–535. https://doi.org/10.1007/s10584-009-9787-8 (2010).
3. Zhu, Y. *et al.* What can the glasgow declaration on forests bring to global emission reduction?. *Innov.* **3**, 100307 (2022).

4. Gu, Y. Y. *et al.* Vegetation dynamics in response to climate change and human activities in the Hulun Lake basin from 1981 to 2019. *Ecol. Indicat.* https://doi.org/10.1016/j.ecolind.2022.108700 (2022).

5. Li, C. H. *et al.* Persistent effects of global warming on vegetation growth are regulated by water in China during 2001–2017. *J. Clean. Prod.* https://doi.org/10.1016/j.jclepro.2022.135198 (2022).

6. Xu, H. J., Wang, X. P. & Zhang, X. X. Decreased vegetation growth in response to summer drought in Central Asia from 2000 to 2012. *Int. J. Appl. Earth Observ. Geoinform.* **52**, 390–402. https://doi.org/10.1016/j.jag.2016.07.010 (2016).

7. Wu, D. H. *et al.* Time-lag effects of global vegetation responses to climate change. *Global Change Biol.* **21**, 3520–3531. https://doi.org/10.1111/gcb.12945 (2015).

8. Xu, H. J., Wang, X. P. & Yang, T. B. Trend shifts in satellite-derived vegetation growth in Central Eurasia, 1982–2013. *Sci. Total Environ.* **579**, 1658–1674. https://doi.org/10.1016/j.scitotenv.2016.11.182 (2017).

9. Cao, W. X., Xu, H. & Zhang, Z. Q. Vegetation growth dynamic and sensitivity to changing climate in a watershed in Northern China. *Remote Sens.* https://doi.org/10.3390/rs14174198 (2022).

10. Beck, P. S. A. & Goetz, S. J. Satellite observations of high northern latitude vegetation productivity changes between 1982 and 2008: ecological variability and regional differences (vol 6, pg 045501, 2011). *Environ. Res. Lett.* https://doi.org/10.1088/1748-9326/7/2/029501 (2012).

11. Angert, A. *et al.* Drier summers cancel out the CO2 uptake enhancement induced by warmer springs. *Proc. Natl. Acad. Sci. USA* **102**, 10823–10827. https://doi.org/10.1073/pnas.0501647102 (2005).

12. Wang, H. *et al.* Strength of association between vegetation greenness and its drivers across China between 1982 and 2015: Regional differences and temporal variations. *Ecol. Indicat.* https://doi.org/10.1016/j.ecolind.2021.107831 (2021).

13. Ukkola, A. M. *et al.* Reduced streamflow in water-stressed climates consistent with CO2 effects on vegetation. *Nat. Clim. Change* **6**, 75. https://doi.org/10.1038/nclimate2831 (2016).

14. Keenan, T. F. & Riley, W. J. Greening of the land surface in the world's cold regions consistent with recent warming. *Nat. Clim. Change* **8**, 825. https://doi.org/10.1038/s41558-018-0258-y (2018).

15. Zhao, W. *et al.* Increased association between climate change and vegetation index variation promotes the coupling of dominant factors and vegetation growth. *Sci. Total Environ.* https://doi.org/10.1016/j.scitotenv.2020.144669 (2021).

16. Cai, S. H., Song, X. N., Hu, R. H. & Guo, D. Ecosystem-dependent responses of vegetation coverage on the Tibetan plateau to climate factors and their lag periods. *Isprs Int. J. Geo-Inform.* https://doi.org/10.3390/ijgi10060394 (2021).

17. Luo, Y. & Chen, H. Y. H. Observations from old forests underestimate climate change effects on tree mortality. *Nat. Commun.* https://doi.org/10.1038/ncomms2681 (2013).

18. Upgupta, S., Sharma, J., Jayaraman, M., Kumar, V. & Ravindranath, N. H. Climate change impact and vulnerability assessment of forests in the Indian Western Himalayan region: A case study of Himachal Pradesh, India. *Clim. Risk Manag.* **10**, 63–76. https://doi.org/10.1016/j.crm.2015.08.002 (2015).

19. Wu, G. L., Cheng, Z., Alatalo, J. M., Zhao, J. X. & Liu, Y. Climate warming consistently reduces grassland ecosystem productivity. *Earths Fut.* https://doi.org/10.1029/2020ef001837 (2021).

20. Tao, J. *et al.* Elevation-dependent relationships between climate change and grassland vegetation variation across the Qinghai-Xizang Plateau. *Int. J. Climatol.* **35**, 1638–1647. https://doi.org/10.1002/joc.4082 (2015).

21. Li, L. H. *et al.* Increasing sensitivity of alpine grasslands to climate variability along an elevational gradient on the Qinghai-Tibet Plateau. *Sci. Total Environ.* **678**, 21–29. https://doi.org/10.1016/j.scitotenv.2019.04.399 (2019).

22. van Oijen, M., Bellocchi, G. & Hoglind, M. Effects of climate change on grassland biodiversity and productivity: The need for a diversity of models. *Agron. Basel* https://doi.org/10.3390/agronomy8020014 (2018).

23. Sun, J. *et al.* Toward a sustainable grassland ecosystem worldwide. *Innov.* **3**, 100265 (2022).

24. Shi, Y. F. *et al.* Recent and future climate change in northwest china. *Clim. Change* **80**, 379–393. https://doi.org/10.1007/s10584-006-9121-7 (2007).

25. Zheng, S. *et al.* The trend towards a warmer and wetter climate observed in arid and semi-arid areas of northwest China from 1959 to 2019. *Environ. Res. Commun.* https://doi.org/10.1088/2515-7620/ac39f7 (2021).

26. Zhang, Q. *et al.* Climatic warming and humidification in the arid region of Northwest China: Multi-scale characteristics and impacts on ecological vegetation. *J. Meteorol. Res.* **35**, 113–127. https://doi.org/10.1007/s13351-021-0105-3 (2021).

27. Wang, P., He, J., Zheng, Y. & Zhang, Q. Aridity-wetness Characteristics over Northwest China in Recent 44 Years. *J. Appl. Meteorol. Sci.* **18**, 769–775 (2007).

28. Wang, A., Miao, Y. & Chen, Y. Interdecadal variation of land water budget in Northwest China from 1961 to 2016. *Trans. Atmosph. Sci.* **43**, 953–966 (2020).

29. Shi, Y., Shen, Y. & Hu, R. Preliminary study on signal, impact and foreground of climatic shift from warm-dry to warm-humid in Northwest China. *J. Glaciol. Geocryol.* **24**, 219–226 (2002).

30. Liu, X. M., Zhang, D., Luo, Y. Z. & Liu, C. M. Spatial and temporal changes in aridity index in northwest China: 1960 to 2010. *Theor. Appl. Climatol.* **112**, 307–316. https://doi.org/10.1007/s00704-012-0734-7 (2013).

31. Niu, Q. F. *et al.* Ecological engineering projects increased vegetation cover, production, and biomass in semiarid and subhumid Northern China. *Land Degrad. Dev.* **30**, 1620–1631. https://doi.org/10.1002/ldr.3351 (2019).

32. Chen, C. *et al.* China and India lead in greening of the world through land-use management. *Nat. Sustain.* **2**, 122–129. https://doi.org/10.1038/s41893-019-0220-7 (2019).

33. Wu, Z. Y. *et al.* Climate and drought risk regionalisation in China based on probabilistic aridity and drought index. *Sci. Total Environ.* **612**, 513–521. https://doi.org/10.1016/j.scitotenv.2017.08.078 (2018).

34. Xu, H. J., Zhao, C. Y. & Wang, X. P. Spatiotemporal differentiation of the terrestrial gross primary production response to climate constraints in a dryland mountain ecosystem of northwestern China. *Agric. For. Meteorol.* https://doi.org/10.1016/j.agrformet.2019.107628 (2019).

35. Harris, I., Osborn, T. J., Jones, P. & Lister, D. Version 4 of the CRU TS monthly high-resolution gridded multivariate climate dataset. *Sci. Data* https://doi.org/10.1038/s41597-020-0453-3 (2020).

36. Munoz-Sabater, J. *et al.* ERA5-Land: a state-of-the-art global reanalysis dataset for land applications. *Earth Syst. Sci. Data* **13**, 4349–4383. https://doi.org/10.5194/essd-13-4349-2021 (2021).

37. Buck, A. L. New equations for computing vapor-pressure and enhancement factor. *J. Appl. Meteorol.* **20**, 1527–1532. https://doi.org/10.1175/1520-0450(1981)020%3c1527:Nefcvp%3e2.0.Co;2 (1981).

38. Wang, X. H. *et al.* Spring temperature change and its implication in the change of vegetation growth in North America from 1982 to 2006. *Proc. Natl. Acad. Sci. USA* **108**, 1240–1245. https://doi.org/10.1073/pnas.1014425108 (2011).

39. Zhu, Z. *et al.* Global data sets of vegetation leaf area index (LAI) 3g and fraction of photosynthetically active radiation (FPAR) 3g derived from global inventory modeling and mapping studies (GIMMS) normalized difference vegetation index (NDVI3g) for the period 1981 to 2011. *Remote Sens.* **5**, 927–948 (2013).

40. Beck, H. E. *et al.* Global evaluation of four AVHRR–NDVI data sets: Intercomparison and assessment against Landsat imagery. *Remote Sens. Environ.* **115**, 2547–2563 (2011).

41. Holben, B. N. Characteristics of maximum-value composite images from temporal AVHRR data. *Int. J. Remote Sens.* **7**, 1417–1434. https://doi.org/10.1080/01431168608948945 (1986).

42. Chen, C. *et al.* Identifying critical climate periods for vegetation growth in the northern hemisphere. *J. Geophys. Res. Biogeosci.* **123**, 2541–2552. https://doi.org/10.1029/2018jg004443 (2018).

43. Piao, S. L. *et al.* Changes in vegetation net primary productivity from 1982 to 1999 in China. *Glob. Biogeochem. Cycles* https://doi.org/10.1029/2004gb002274 (2005).
44. Liu, H. *et al.* Annual dynamics of global land cover and its long-term changes from 1982 to 2015. *Earth Syst. Sci. Data* **12**, 1217–1243. https://doi.org/10.5194/essd-12-1217-2020 (2020).
45. Tian, F. Q. *et al.* Exploring spatio-temporal patterns of sediment load and driving factors in Lancang-Mekong River basin before operation of mega-dams (1968–2002). *J. Hydrol.* https://doi.org/10.1016/j.jhydrol.2022.128922 (2023).
46. Zha, X. N., Xiong, L. H., Liu, C. K., Shu, P. & Xiong, B. Identification and evaluation of soil moisture flash drought by a nonstationary framework considering climate and land cover changes. *Sci. Total Environ.* https://doi.org/10.1016/j.scitotenv.2022.158953 (2023).
47. Han, Q. Q. *et al.* Global long term daily 1 km surface soil moisture dataset with physics informed machine learning. *Sci. Data* https://doi.org/10.1038/s41597-023-02011-7 (2023).
48. Baba, K., Shibata, R. & Sibuya, M. Partial correlation and conditional correlation as measures of conditional independence. *Aust. New Zealand J. Stat.* **46**, 657–664. https://doi.org/10.1111/j.1467-842X.2004.00360.x (2004).
49. Song, Y. & Ma, M. G. A statistical analysis of the relationship between climatic factors and the Normalized Difference Vegetation Index in China. *Int. J. Remote Sens.* **32**, 3947–3965. https://doi.org/10.1080/01431161003801336 (2011).
50. Yu, H. C., Bian, Z. F., Mu, S. G., Yuan, J. F. & Chen, F. Effects of climate change on land cover change and vegetation dynamics in Xinjiang, China. *Int. J. Environ. Res. Public Health* https://doi.org/10.3390/ijerph17134865 (2020).
51. Huxman, T. E. *et al.* Convergence across biomes to a common rain-use efficiency. *Nature* **429**, 651–654 (2004).
52. Maurer, G. E., Hallmark, A. J., Brown, R. F., Sala, O. E. & Collins, S. L. Sensitivity of primary production to precipitation across the United States. *Ecol. Lett.* **23**, 527–536 (2020).
53. Piao, S. L., Friedlingstein, P., Ciais, P., Zhou, L. M. & Chen, A. P. Effect of climate and CO2 changes on the greening of the Northern Hemisphere over the past two decades. *Geophys. Res. Lett.* https://doi.org/10.1029/2006gl028205 (2006).
54. Huang, M. *et al.* Air temperature optima of vegetation productivity across global biomes. *Nat. Ecol. Evol.* **3**, 772–779 (2019).
55. Xu, L. *et al.* Temperature and vegetation seasonality diminishment over northern lands. *Nat. Clim. Change* **3**, 581–586 (2013).
56. Piao, S. L. *et al.* Evidence for a weakening relationship between interannual temperature variability and northern vegetation activity. *Nat. Commun.* https://doi.org/10.1038/ncomms6018 (2014).
57. D'Arrigo, R. D. *et al.* Thresholds for warming-induced growth decline at elevational tree line in the Yukon Territory, Canada. *Global Biogeochem. Cycle* https://doi.org/10.1029/2004gb002249 (2004).
58. Yuan, W. P. *et al.* Increased atmospheric vapor pressure deficit reduces global vegetation growth. *Sci. Adv.* https://doi.org/10.1126/sciadv.aax1396 (2019).

Acknowledgements

Author contributions

Shijun Zheng, Dailiang Peng and Bing Zhang designed the research ideas. Shijun Zheng and Yan Wang completed the code for analysis. Yuhao Pan, Xuxiang Feng and Changyong Dou prepared the NDVI and climate data. Le Yu helped with the preparation of the land cover datasets. All authors commented on the paper and provided feedback throughout the data analysis.

Competing interests

The authors declare no competing interests.

Additional information

Supplementary Information The online version contains supplementary material available at https://doi.org/10.1038/s41598-024-68066-7.

Correspondence and requests for materials should be addressed to D.P. or L.Y.

Reprints and permissions information is available at www.nature.com/reprints.

Publisher's note Springer Nature remains neutral with regard to jurisdictional claims in published maps and institutional affiliations.